Electronic band structures and x-ray photoelectron spectra of ZrC, HfC, and TaC

Hideo Ihara, Masayuki Hirabayashi, and Hiroshi Nakagawa
Electrotechnical Laboratory, Tanashi, Tokyo, Japan
(Received 12 February 1976)

The band structures and densities of states (DOSs) of ZrC, HfC, and TaC were calculated by the augmented-plane-wave method, and the x-ray photoelectron spectra of valence bands of these compounds were observed. The theoretical energy distribution curves (EDCs) were in good agreement with the experimental EDCs. These band structures resemble each other and also those of TiC obtained by our previous work. This fact suggests that the rigid-band model is applicable to the transition-metal carbides with the rock-salt structure. Their DOSs are divided into three parts. Peak I derived from the C $2s$ state is isolated from the higher valence-band peak II arising from the C $2p$ and the valence electrons of the metal atom. Peak III derived from the d and s states of the metal atom is separated by the Fermi level from peak II. The Fermi level lies at the minimum point of the DOS for the group IV carbides, but for TaC it lies at a relatively large DOS point. The DOS at the Fermi level of ZrC, HfC, and TaC are 0.18, 0.16, and 0.65 electrons/(eV primitive cell), respectively. The characteristic mutual differences among these compounds are a stronger localization of d electrons in ZrC and HfC compared with TiC and an enhancement of the photoelectron spectrum intensity of TaC around the Fermi level.

I. INTRODUCTION

Transition-metal carbides have aroused theoretical and practical interest in their extremely high melting point, hardness, metallic property, and superconductivity. These unique properties are thought to connect closely with their unique electronic structures and chemical-bonding characters. An intensive investigation of the band structure has been performed for TiC,[1-3] VC,[4,5] and NbC.[6,7] For ZrC, HfC, and TaC works concerned with the band structure such as measurements of x-ray emission[8-10] and low-temperature specific heat,[11] calculations of the band structure and density of states (DOS) of ZrC,[12,13] and the DOSs at the Fermi level of HfC and TaC,[14] have been reported. These works are, however, not sufficient to derive the definite band structures and DOSs of ZrC, HfC, and TaC. The band structure of ZrC recently calculated by Alward *et al.*[13] contradicts the result of Potoracha *et al.*,[12] especially in the energy of the lowest band derived from the C $2s$ state and the position of the Γ'_{25} point relative to the Fermi level. Hence more intensive experimental and theoretical studies are necessary to clarify the electronic structures of ZrC, HfC, and TaC.

The present paper is an extension of our previous work[3] on TiC to other transition-metal carbides. The previous paper has shown that the band structure of TiC from the augmented-plane-wave (APW) calculation is consistent with the x-ray photoelectron spectrum and can explain satisfactorily other experimental results such as x-ray emission and absorption, optical reflectance, and low-temperature specific heat. The interplay of the APW calculation and the photoemission measurement using monochromatic x rays (XPS) seems to be most rewarding for the investigation of the electronic band structure of the transition-metal carbides. In this work the band structures and the DOSs of ZrC, HfC, and TaC were calculated by the APW method, and the XPS valence-band spectra of these compounds were observed. The theoretical band structures and DOSs were compared with the XPS spectra and other available works, and good results were obtained. From these results it is verified that the band structure and the bonding character of the transition-metal carbides can be consistently explained with the idea obtained for TiC.

A variety of band-structure models have been proposed previously to explain the physical properties of the transition-metal carbides. The former ideas can be attributed to two distinct models.[11] The first model stresses the importance of metal-metal bonds and the interstitial nature of carbon in explaining the observed properties of these materials. The second model attributes these properties to the metal-carbon bonds. The difference in these models depends on the relative placement of the energy of the C $2p$ state. When the band arising from the C $2p$ state is low in energy relative to the Fermi level, strong bonding occurs between the C $2p$ electrons and the d electrons of the metal atom. This concept of bonding supports the idea of a strongly localized or covalent bond and is used to explain the octahedral configuration, hardness, and brittleness of these compounds. In the opposite approach, the C $2p$ state is placed high in energy relative to the Fermi level and is not occupied. The bonding is primarily between metal atoms, and the valence-

band structure resembles that of the pure-transition-metal elements. This approach is good in accounting for the high melting points, metallic properties, and wide range of vacancy concentration.

The recent theories of bonding for the transition-metal carbides have emphasized both the metal-carbon and metal-metal bonding and proposed a simultaneous contribution from metallic, covalent, and ionic bonds to the cohesive energy.[11] Our previous work has proposed the bonding model of TiC,[3] as follows: (i) The C $2p$ state and a fraction of Ti $3d$ state form hybrid states below the Fermi level and contribute to the covalent bond between the carbon and titanium atoms. (ii) TiC is a semimetal compound, and conduction electrons from the Ti $3d$ and C $2p$ states contribute to metallic bonding. (iii) The Ti $4s$ electrons diffuse to the Ti $3d$ and C $2p$ states and the charge transfer from metal to carbon occurs mainly between the Ti $4s$ and C $2p$ states, which contributes to the ionic bond. (iv) The C $2s$ state makes a small contribution to the bonding of carbon and titanium and sp^3 hybridization of the carbon atom. (v) The carbon atom does not form the sp^3 hybrid orbital, thus three C $2p$ orbitals determine the atomic configuration around the carbon atom, which is consistent with the rock-salt structure of TiC. This bonding model is expected to be applicable to other groups-IV and -V transition-metal carbides with rock-salt structure except that conduction electrons of the group-V transition-metal carbides are derived predominantly from the d electrons of the metal atom.

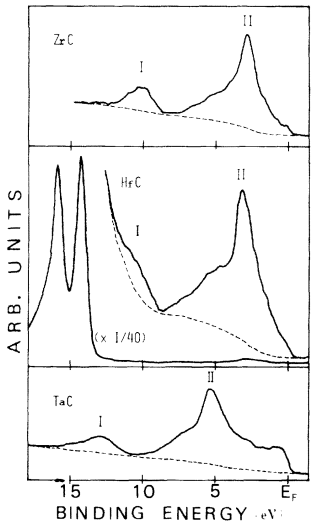

FIG. 1. X-ray photoelectron spectra of the valence band of ZrC, HfC, and TaC. Dashed lines show backgrounds.

The present work shows that the band structures of TiC, ZrC, HfC, and TaC have quite a lot in common and that the idea of the bonding character of TiC holds true for ZrC, HfC, and TaC. This leads to the assumption that the rigid-band model is a good approximation for the transition-metal carbides with the rock-salt structure. This fact would be considerably helpful for the investigation of the band structure and physical properties of nonstoichiometric compounds and mutual solid solutions of these materials.

In Sec. II of this paper XPS measurement of ZrC, HfC, and TaC and their results are described. In Sec. III, the band structures and DOSs of these compounds are calculated by the APW method. The theoretical energy distribution curves (EDCs) are compared with the experimental EDCs in Sec. IV A, and the present results are discussed in relation to previous works in Sec. IV B. In Sec. V, a summary is given.

II. EXPERIMENT AND RESULTS

The samples of transition-metal carbides were prepared by hot-pressing powders of monocarbides in graphite dies at temperature of 2600 °C and 300 kg/cm^2 in an atmosphere below 1×10^{-3} Torr for 1 h. The ratios of combined carbon to metal atoms of the powders were above 0.98. The relative densities of the samples of ZrC, HfC, and TaC were 0.99, 0.90, and 0.93, respectively.[15] After hot pressing the samples were polished and inserted into the analyzing chamber of an HP 5950A ESCA spectrometer with a resolution of 0.6 eV. The sample treatment and the measurement procedure were described elsewhere in detail.[3]

Figure 1 reproduces the valence-band photoemis-

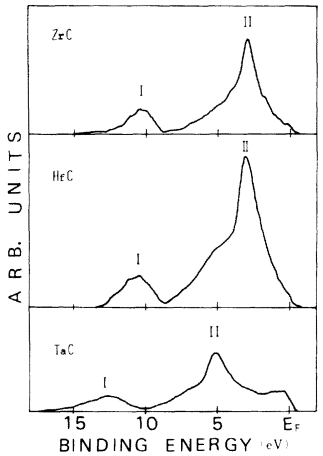

FIG. 2. Corrected x-ray photoelectron spectra obtained by subtracting the background.

TABLE I. Characteristic features of the x-ray photoelectron spectra of ZrC, HfC, and TaC.

Compound	Binding energy (eV) Peak I	Peak II	Energy difference between peaks I and II (eV)	Full width at half-maximum (eV) Peak I	Peak II	Ratio of the integrated intensity of peak II to I
TiC	10.7	3.4	7.3	3.2	3.7	2.9 : 1
ZrC	10.3	3.0	7.3	2.1	1.7	4.6 : 1
HfC	10.5	3.2	7.3	2.6	2.1	6.2 : 1
TaC	12.5	5.2	7.2	3.0	2.4	4.5 : 1

sion spectra of ZrC, HfC, and TaC without any correction. The accumulation times for these spectra were 20 h. Two predominant peaks marked I and II appear in the valence-band region as in the case of TiC.[3] In the spectrum of HfC, the C $2s$ (peak I) and Hf $4f_{7/2}$ overlap. The contribution of the Hf $4f$ peak to the valence-band spectrum can be estimated by referring to that of the Ta $4f$ peak. A dashed line in each spectrum shows a background from inelastically scattered electrons which is proportional to the spectrum intensity integrated from the Fermi level to the considered point. The contribution of surface contaminants to the EDCs in the region of the valence band was of the level of a background.

The corrected XPS spectra in Fig. 2 were obtained by subtracting the background from the experimental spectra. The spectra of ZrC and HfC resemble each other, and they are shaped like the EDC of TaC below 2 eV from the Fermi level. The binding energies, energy differences between peaks I and II, the full widths at half-maximum (FWHMs) and ratios of the integrated intensity of peak II to I in these spectra are listed in Table I together with those of TiC. The binding energies of peaks I and II of the group IV metal carbides are nearly equal to each other, but they decrease a little by a step of 0.2 eV going from TiC to HfC and ZrC. The energy differences between peaks I and II are equal to each other and are almost equal to that for TaC. Both peaks I and II of TaC are located on a lower energy side than those of HfC by 2.0 eV, which is caused by the Fermi-level shift due to a surplus valence electron of TaC.

The FWHMs of those peaks are considerably different from each other. The tendency of peak I to sharpen parallels that of peak II. For the group-IV carbides this tendency is the same as the tendency of the binding energies of peaks I and II to decrease, and it is on the order of the increase of the lattice constants.[11] Both peaks of ZrC are the sharpest, and the FWHM of peak II to which d electrons contribute is about $\frac{1}{2}$ that of TiC. The FWHMs of both peaks of TaC have a place between those of HfC and TiC. The ratios of peak II to peak I in the integrated intensity increase from TiC to ZrC and HfC and go up from a ratio of six electrons for C $2p^2$ and metal-atom nd^2 and $(n+1)s^2$ configurations to two electrons for C $2s^2$. The spectrum intensity of TaC at the Fermi edge is considerably larger compared with those of the group-IV carbides. This would partly reflect a larger DOS at the Fermi level in TaC.

III. BAND CALCULATIONS

The APW method is expected to be the most promising approach to the electronic band structures of the transition-metal carbides.[3] The present calculations were performed by using the same procedure as in the case of TiC.[3] The relativistic

TABLE II. Electronic configuration, lattice constant, and potential parameter used in the band calculation of ZrC, HfC, and TaC in atomic units.

Compound	Electronic configuration	Lattice parameter (a.u.)	APW sphere radius (a.u.)	Constant part of potential (Ry)
ZrC	C $2s^2 2p^2$; Zr $4d^2 5s^2$	8.8567	C : 1.822; Zr : 2.586	−1.7325
HfC	C $2s^2 2p^2$; Hf $5d^2 5s^2$	8.7707	C : 1.733; Hf : 2.586	−1.7475
TaC	C $2s^2 2p^2$; Ta $5d^3 5s^2$	8.4211	C : 1.733; Ta : 2.460	−1.8995

effect was not considered even for HfC and TaC. The potentials of the constituent atoms were obtained from the neutral-atomic-charge densities with the program of Herman and Skillman,[16] and the Slater exchange potential was employed. The valence electronic configurations and relevant potential parameters are listed in Table II. The convergences of the band energies were within 0.01 Ry. The band energies were calculated on a grid of 89 points in $\frac{1}{48}$ of the Brillouin zone to derive the DOS. It was verified for TiC that the DOS obtained by using a grid of 89 points was not different in the characteristic features from that obtained by using a grid of 222 points.

The calculated band structures of ZrC, HfC, and TaC closely resemble each other as shown in Fig. 3 and also resemble those of TiC. This fact suggests that the rigid-band model can be a good approximation for transition-metal carbides with rock-salt structure. The energy bands of these compounds can be commonly explained in a way similar to that for TiC.

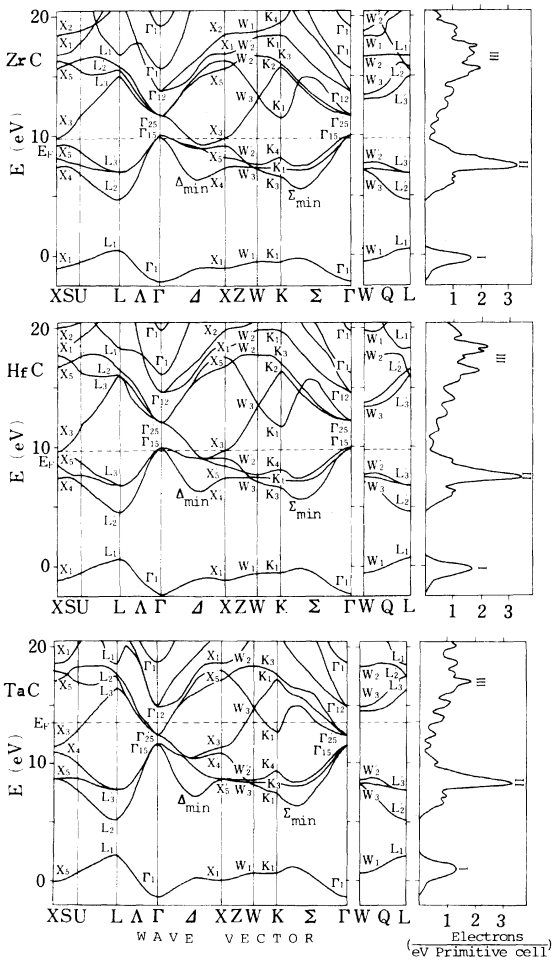

FIG. 3. Band structures and densities of states of ZrC, HfC, and TaC.

Band 1 (being numbered from the lowest energy side) corresponds to the C 2s state in every compound, and forms an isolated peak marked I corresponding to the energy of 0 eV in the DOS spectra. This band is separated by more than 3.0 eV from the higher band, from which one infers that the carbon atom does not form the sp^3 hybrid state and the C 2s state makes few contributions to the bonding of the carbon and metal atoms as in TiC. The points Γ_1 and L_1 of this band correspond to the lower edge and the upper edge of peak I, respectively. The flat part of this band from X_1 to K_1 over the surface of the Brillouin zone gives rise to the top of the peak.

The three bands 2 to 4, degenerate at the Γ_{15} point, arise mainly from the C 2p state and partially from the metal d state. The upper three bands 5 to 7 degenerate at Γ'_{25} and the two bands 8 to 9 degenerate at Γ_{12} arise mainly from the metal d_ϵ and d_γ states, respectively. The band 5 from the metal d_ϵ state goes down from the Γ'_{25} point along the symmetry line Δ and closes to or overlaps with the band 4 from the C 2p state between the Γ and X points. The mixture of the C 2p and the metal d_ϵ states forms the large peak II. These facts mean a large contribution of covalent bonds between the C 2p and the metal d states to the cohesive energy of the transition-metal carbides. The top of peak II corresponds to the near degeneracy of the bands 3 and 4 around the symmetry points L and W on the Brillouin zone. A shoulder on the lower-energy side of the peak corresponds to the flat part around $\Delta_{\min}$ and $\Sigma_{\min}$ of band 2. The lowest point L'_2 of band 2 corresponds to the bottom of peak II.

The Fermi level of the group-IV transition-metal carbides intercepts the four bands 2 to 5 derived from the C 2p and metal d states. The slope of these bands at the Fermi level is relatively sharp and only band 5 exists between the energy levels of the Γ_{15} and Γ'_{25} points. Thus the Fermi level of the group-IV transition-metal carbides lies at one of the minimum points of the DOS between peaks II and III. The other minimum of the DOS is located at about 1 eV above the Fermi level. The DOSs at the Fermi level of ZrC and HfC are 0.18 and 0.16 electrons/(eV primitive cell), respectively. The Fermi level of TaC is located at the relatively large DOS point between the Γ'_{25} and Γ_{12} points and intercepts the three bands 5 to 7 derived from the Ta 5d state. The DOS at the Fermi level of TaC is 0.65 electrons/(eV primitive cell), which is larger than that of HfC by a factor of about 4 and favors a high-superconducting transition temperature.

TABLE III. Characteristic features of calculated densities of states of ZrC, HfC, and TaC.

Compound	Binding energy (eV) Peak I	Peak II	Energy difference between peaks I and II (eV)	Full width at half-maximum (eV) Peak I	Peak II	DOS at the Fermi level [electrons/(eV primitive cell)]
TiC	10.6	2.9	7.7	1.4	3.4	0.22
ZrC	10.2	2.5	7.7	1.1	1.2	0.18
HfC	10.1	2.4	7.7	1.1	1.1	0.16
TaC	12.6	5.3	7.3	1.4	1.1	0.65

The five bands 5 to 9, mainly derived from the metal *d* state, form the broad peak III between 14 and 20 eV. The conduction *d* bands of ZrC, HfC, and TaC broaden and lose the characteristic features of peak III with a shoulder S_{III} which appears in the DOS of TiC.[3] The metal outermost *s* state contributes to band 10 at the Γ_1 point which lies above the Fermi level, so that the electronic charge in this state is forced to diffuse to the metal *d* state and the C 2*p* state. Therefore the charge transfer from the metal outermost *s* state to the C 2*p* state occurs in the transition-metal carbides, and an ionic bond contributes partially to their cohesive energy. The upper band 11 is attributable to the C 3*s* state. The bands 10 and 11 of ZrC, HfC, and TaC are lower in energy in comparison with those of TiC. The band structures above 20 eV of ZrC, HfC, and TaC which were not calculated could be inferred from the result for TiC by using the rigid-band model.

The DOSs of those compounds resemble each other in the region of the valence band, except for the increase of the Fermi energy in TaC. The DOSs in the region of the conduction band are somewhat different from each other. The relative weight of the DOS shifts to the higher-energy side going from TiC to ZrC and HfC. The theoretical binding energies and FWHMs of peaks I and II and the DOSs at the Fermi level are tabulated in Table III for these compounds. The binding energies of peaks I and II of ZrC and HfC almost coincide, but are higher than those of TiC by about 0.4 eV. This energy difference is nearly equal to the experimental binding energy difference of 0.4 eV between TiC and ZrC for both peaks I and II. The energies of peaks I and II of TaC are lower than those of the group-IV carbides by about 2.5 eV owing to the contribution of an extra valence *d* electron. The energy differences between peaks I and II of the group-IV carbides equal each other and are nearly equal to that for TaC.

The FWHMs of peak I of both ZrC and HfC are equal, but are smaller than those of TiC and TaC. The FWHMs of peak II of ZrC, HfC, and TaC are nearly equal, but smaller than that of TiC by a factor of 3. This suggests that the *d* electrons of ZrC, HfC, and TaC are more strongly localized in comparison with TiC.

IV. DISCUSSIONS

A. Comparison between experiment and calculation

The theoretical EDCs were obtained from the above-mentioned DOSs by assuming a Lorentzian smearing function with a FWHM of 0.6 eV. Figure 4 shows a comparison between the corrected XPS spectra (solid line) and the theoretical EDCs (dashed line) for ZrC, HfC, and TaC. These spectra are not normalized. The characteristic features of the theoretical EDCs can be related to the corresponding features of the experimental EDCs.

The agreement of the binding energies of peak I derived from the C 2*s* state is good between the experimental and theoretical EDCs in every compound. Peak II of the group-IV carbides which is derived from the C 2*p* state and the metal *d* electrons is located at a little lower energy in the ex-

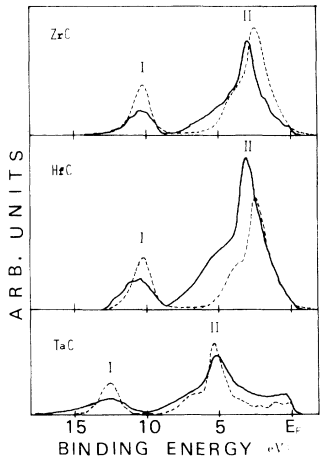

FIG. 4. Comparison between the experimental energy distribution curves (solid lines) and the theoretical ones (dashed lines) of ZrC, HfC, and TaC.

perimental EDC than in the theoretical EDC. In the EDC of TaC, however, the coincidence of the position of both the peaks is very good. As regards the FWHMs of peaks I and II, the experimental ones are larger than the theoretical ones by a factor of about 2. The peak broadening in the XPS EDC is partly attributable to the lifetime broadening as in the case of TiC.

Fine structures observed around the Fermi edge in the experimental EDCs of ZrC and HfC are smeared out in the theoretical EDCs, while the fine structure of TaC is more discernible in the theoretical EDC than in the experimental one. The characteristic difference between the experimental and theoretical EDCs of TaC is that the spectrum's intensity around the Fermi edge is considerably enhanced. This enhancement corresponds to the increase of the contribution of the Ta 5*d* electrons to the DOS around the Fermi level. A large transition probability of the *d* electron irradiated with the Al $K\alpha$ line would be related to this phenomenon.

The increase in intensity of peak II accompanied with sharpening can be related to the localization of the *d* electrons of the metal atom. This localization phenomenon is reflected in the fact that the ratios of peak II to I in the integrated intensity remarkably increase from TiC to ZrC (see Table I). The localization of the *d* electrons presumably changes the character of the bonding between the carbon and metal atoms. This localization might be associated with the extremely high melting points of HfC and TaC, and inversely, delocalization might be associated with the extreme hardness of TiC.

The disagreement between the experimental and theoretical FWHMs of peak II in HfC and TaC would be partly caused by spin-orbit interaction. Its effect, however, would not be predominant, because the disagreement for peak I is in the same direction as for peak II and this disagreement is also observed for ZrC in which the spin-orbit interaction is small.[16] In order to settle the disagreement between the experimental and theoretical EDCs in the FWHMs and the binding energies, a greatly improved band calculation taking into consideration the transition probability would be necessary.

B. Comparison with other works

Present results can be compared with other available data such as x-ray emission spectra, low-temperature specific heats, magnetic susceptibility, band structures, and DOSs. A series of C K-emission spectra of the transition metal-carbides was observed by Holliday.[8] In those spectra the peak arising from the valence electrons of the metal atom and the C 2*p* state are observed, but the peak arising from the C 2*s* state is not observed owing to the selection rule. As the Fermi edge is not indicated in those spectra, if the position of the Fermi edge is determined by the leading edge of each spectrum, the binding energy of each peak is estimated at about 3.0 eV for ZrC and HfC, and 5.2 eV for TaC. These results are in good agreement with the results of XPS (see Table I), the TaC spectrum especially has features similar to those of peak II of its XPS spectrum. The FWHMs of those peaks are 2.4, 3.0, and 3.0 eV for ZrC, HfC, and TaC, respectively. Though these values are larger than the results of XPS, the FWHM of ZrC is smallest as in the XPS spectra. The difference in FWHMs between x-ray emission and XPS spectra would be partly caused by the differences of the selection rule and the resolution of the apparatus.

The Zr M_V-emission spectrum of ZrC obtained by Nemoshkalenko *et al.*[10] gives a FWHM of 2.8 eV for the peak corresponding to peak II in this work. That peak contains a small hump on the high-energy side like our results, but their Zr $L\beta_2$-emission spectrum shows a broad and symmetrical peak. These peaks lie too far from the Fermi edge compared with our results, which would be caused by an experimental condition. The Zr L_{III}-emission spectrum of ZrC observed by Ramqvist *et al.*[9] cannot be used for a comparison

TABLE IV. Comparison between calculated densities of states at the Fermi level [electrons/(eV primitive cell)].

Compound	Present work	Klein and Papaconstantopoulos (Ref. 14)	Alward *et al.* (Ref. 13)	Potoracha *et al.* (Ref. 12)
TiC	0.22 (Ref. 3)		0.242	
ZrC	0.18		0.182	0.32
HfC	0.16	0.13		
TaC	0.65	0.66		(0.50) from NbC

with the DOS of ZrC, because this spectrum is too broad and the position of the Fermi edge is not discernible.

The low-temperature specific-heat data[11] for ZrC, HfC, and TaC give larger DOSs at the Fermi level than our calculation by a factor of about 2. The DOS of TaC estimated by Zeller[17] from specific-heat data with correction for electron-phonon interaction is reduced to 0.72 electrons/(eV primitive cell) and close to our result. Borukhovich *et al.*[18] estimated the DOS at the Fermi level for ZrC from the observed magnetic susceptibility at 0.2 electrons/(eV primitive cell) which is nearly equal to our results.

The calculated DOSs at the Fermi level were obtained for HfC, NbC, and TaC from a self-consistent APW calculation by Klein and Papaconstantopoulos,[14] for ZrC, VC, and NbC from the tight-binding method by Potoracha *et al.* (PTG),[12] and for TiC and ZrC from a modified empirical-pseudopotential method by Alward *et al.* (AFEW).[13] The calculated DOS at the Fermi level is tabulated in Table IV. Our results are in good agreement with those obtained by Klein and Papaconstantopoulos and AFEW, but not with the values obtained by PTG.

The band structure and DOS of ZrC were calculated by PTG[12] and AFEW.[13] Their histograms of DOS are reproduced in Fig. 5 together with the present DOS curve. The binding energy of peak I after PTG (long-interval histogram in Fig. 5) is 10.7 eV, which is close to 10.3 from the XPS measurement and 10.2 from the present calculation. Peak I of PTG is, however, asymmetric and is not shaped like the peak of the XPS spectrum. The band energy corresponding to peak I obtained by AFEW is about 20 eV which is quite different from the present result. The binding energies of peak II after PTG and AFEW (short-interval histogram in Fig. 5) are 1.7 and 3.8 eV, respectively. The present calculated value is 2.5 eV, which falls in near the middle point between their values. The value of AFEW is closer to the 3.0 eV of the XPS

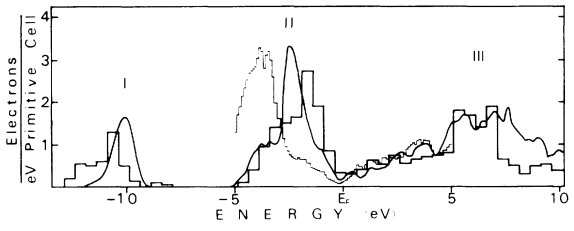

FIG. 5. Comparison of the calculated densities of states of ZrC between the present work (solid line), Potoracha *et al.* (Ref. 12) (long-interval histogram) and Alward *et al.* (Ref. 13) (short-interval histogram).

measurement than that of PTG. In the band structure of AFEW, however, the Γ'_{25} point lies below the Fermi level, and as a whole the valence band seems to be too low in energy. The degenerate point of bands 3, 4, and 5 at the Γ point must locate above the Fermi level as in the cases of our work and PTG's. This would be one of the reasons for the fact that most of the structures of the reflectivity of ZrC and TiC are not closely associated with the critical point.[13] The FWHM of peak II obtained by AFEW and PTG are 2.0 and 2.5 eV, respectively, and the former is close to the result of XPS. As regards the features of peak II, however, the result of PTG is rather good, because the slope of peak II is steep on the high-energy side and gentle on the low-energy side as in the XPS spectrum.

Among the three band calculations for ZrC, the present result from the APW calculation is in the best agreement with the result of XPS. The result from the tight-binding method after PTG is relatively good, though the DOS at the Fermi level is too large and the binding energy of peak II is small. The partial DOSs corresponding to each atomic states were calculated by PTG. Their calculation shows that the C 2*s* state predominantly contributes to peak I, the C 2*p* state mainly contributes to peak II and partially to peak III, and the Zr 4*d* state mainly to peak III and partially to peak II. These results are consistent with the present calculation.

The agreement between the three calculated DOSs of PTG, AFEW, and ours is relatively good in the region of the conduction band. However, the ordering of the degenerate bands at the Γ point is different among the three kinds of band structures. Our result is of the order of $\Gamma_{15} - \Gamma'_{25} - \Gamma_{12}$, while PTG's is of the order of $\Gamma'_{25} - \Gamma_{15} - \Gamma_{12}$ and AFEW's of $\Gamma'_{25} - \Gamma_{12} - \Gamma_{15}$. From symmetry considerations, our result leads to a $p - d_\epsilon - d_\gamma$ ordering of the electronic states, and PTG's leads to $d_\epsilon - p - d_\gamma$ and AFEW's leads to $d_\epsilon - d_\gamma - p$. These different results imply three types of charge-transfer model. The first is the charge transfer from the metal to the carbon atom, the second is a small charge transfer, and the third is conversely from the carbon to the metal atom. Our result of the charge transfer from the metal to the carbon atom is consistent with the result of the core-level chemical shift from XPS measurement.[19]

At the end of the discussion it is speculative to note the golden color of the TaC specimen. The band structure of TaC shows that the interband transition between the Γ'_{25} and Γ_{12} bands is 2.45 eV which is equal to the onset of the absorption band of gold.[20] Thus the blue light is absorbed and the other visible light is reflected. This would be an

origin of the golden color of TaC. Now, optical measurement is under current investigation.

V. SUMMARY

The valence-band spectra of ZrC, HfC, and TaC were observed by XPS, and the band structures and DOSs of these compounds were calculated by the APW method. The theoretical EDCs are in good agreement with the XPS spectra. The experimental and theoretical EDCs are consistent with the C K-emission spectra obtained by Holliday. The calculated DOSs at the Fermi level of ZrC, HfC, and TaC are 0.18, 0.16, and 0.65 electrons/(eV primitive cell), respectively, which are in good agreement with the results calculated by Klein and Papaconstantopoulos and Alward *et al.* The large DOS at the Fermi level of TaC contributes favorably to its superconductivity. The XPS spectrum of ZrC is in better agreement with the present result from the APW calculation than other results obtained by Potoracha *et al.* from the tight-binding method and by Alward *et al.* from a pseudopotential method.

The band structures of TiC, ZrC, HfC, and TaC have many features in common, which suggests that the rigid-band model will be a good approximation for the transition-metal carbides with the rock-salt structure. This fact allows us to apply the bonding model of TiC described in Sec. I to other transition-metal carbides. These results are expected to be useful to explain both the bonding character and the physical properties of nonstoichiometric compounds and solid solutions of transition-metal carbides.

There are, however, some differences among their band structures. These differences are considered to be closely related to the peculiarities in such physical properties as melting point, hardness, and superconductivity of the transition-metal carbides. The intensity of peak II relative to peak I increases from TiC to ZrC and HfC in the XPS spectra. This fact is thought to reflect the localization of the d electrons. The localization phenomenon might be related to the extremely high melting point of the transition-metal carbides, and inversely the delocalization of the d electrons might be related to their hardness. Although the band structures and DOSs of HfC and TaC resemble each other, their XPS spectra are different, especially around the Fermi level. The enhancement of the XPS spectrum intensity around the Fermi level of TaC is associated with the contribution of Ta $5d$ electrons to the conduction electrons. The golden color of TaC is caused by the optical absorption of the interband transition around the Γ point.

ACKNOWLEDGMENTS

The authors gratefully appreciate A. Itoh, Y. Kumashiro, N. Nagaoka and T. Sugita for stimulating and valuable suggestions and discussions.

[1]V. Ern and A. C. Switendick, Phys. Rev. 137, A1927 (1965).
[2]J. B. Conklin, Jr. and D. J. Silversmith, Int. J. Quantum Chem. 25, 243 (1968).
[3]H. Ihara, Y. Kumashiro, and A. Itoh, Phys. Rev. B 12, 5465 (1975).
[4]A. Neckel, P. Rastl, P. Weinberger, and R. Mechtler, Theor. Chim. Acta 24, 170 (1972).
[5]J. Zbasnik and L. E. Toth, Phys. Rev. B 8, 452 (1973).
[6]J. B. Conklin, Jr., F. W. Averill, and T. M. Hattox, J. Phys. (Paris) Suppl. 33, C3-2131 (1972).
[7]D. J. Chadi and M. L. Cohen, Phys. Rev. B 10, 496 (1974).
[8]J. E. Holliday, in *Advances in X-ray Analysis*, edited by B. L. Henke, J. B. Newkirk, and G. R. Mallett (Plenum, New York, 1970), Vol. 13, p. 136.
[9]L. Ramqvist, B. Ekstig, E. Källne, E. Noreland, and R. Manne, J. Phys. Chem. Solids 32, 149 (1971).
[10]V. V. Nemoshkalenko, V. P. Krivitskill, A. P. Nesenjuk, L. I. Nikolajev, and A. P. Shpak, J. Phys. Chem. Solids 36, 277 (1975).
[11]L. E. Toth, *Transition Metal Carbides and Nitrides* (Academic, New York, 1971).
[12]V. I. Potoracha, V. A. Tskhai, and P. V. Geld, Phys. Status Solidi B 48, 119 (1971).
[13]J. F. Alward, C. Y. Fong, M. El-Batanouny, and F. Wooten, Phys. Rev. B 12, 1105 (1975).
[14]B. M. Klein and D. A. Papaconstantopoulos, Phys. Rev. Lett. 32, 1193 (1974).
[15]M. Hirabayashi and H. Nakagawa (unpublished).
[16]F. Herman and S. Skillman, *Atomic Structure Calculations* (Prentice-Hall, Englewood Cliffs, N. J., 1963).
[17]H. Z. Zeller, Phys. Rev. B 5, 1813 (1972).
[18]A. S. Borukhovich, L. B. Dubrouskaya, I. I. Matveenko, and P. V. Geld, Phys. Status Solidi 36, 97 (1969).
[19]L. Ramqvist, Jernkontorets Ann. 153, 159 (1969), and the author's unpublished work.
[20]C. Kittel, *Introduction to Solid State Physics*, 2nd ed., (Wiley, New York, 1956), p. 319.